Volume 1 | Number 1 | Jan 2013 | Pages 1–100

Journal of
Materials Chemistry A

Materials for energy and sustainability
www.rsc.org/materialsA

Li⁺

ROYAL SOCIETY
OF CHEMISTRY

ROYAL SOCIETY
OF CHEMISTRY

www.rsc.org/materialsA

Journal of Materials Chemistry A

ARTICLE

Ultrasensitive Single Crystalline TeO$_2$ Nanowire Based Hydrogen Gas Sensor

Changzeng Yan,[a] Binh Le Huy[b] and Dae Joon Kang*[a]

We report a high performance tellurium dioxide (TeO$_2$) nanowire (NW)-based hydrogen gas sensor fabricated by a standard photolithography. High-quality single crystalline TeO$_2$ NWs were synthesized using gold as a catalyst with high reproducibility. The resulting NW diameters were as small as 30 nm. The gas sensing properties were investigated at various temperatures under two different H$_2$ concentrations (0.5% and 1%). We observed $\Delta R/R$ responses of 28% and 57% at 25 °C and 140 °C, respectively. Furthermore, detailed sensitivity-versus-temperature analysis shows that sensitivity of up to 138% can be obtained at 140 °C for 1% H$_2$ concentration.

Introduction

The development of highly sensitive, selective, cost-effective, reliable, and compact gas-sensing devices for detecting combustible, carcinogenic, chemical agents and toxic chemicals is of major importance.[1] Over the last several decades, bulk and thin film metal oxides have been widely studied and used to sense gas species, acetone, humidity, and more.[2-4] In recent years, there has been great interest in 1D metal oxide nanostructures for gas sensor applications[4] because they are low cost, robust, compact, long lasting and have high sensitivity and quick response times. There are many wide bandgap semiconducting materials that have been reported as potential gas sensors, such as WO$_3$, SnO$_2$ and Fe$_2$O$_3$.[5-9] However, these gas sensors can only be operated above 200 °C, which results in large power consumption and complexities in integration.[10-12] Additionally, these gas sensors are not very sensitive when they work at high temperature, affecting the stability and lifetime of devices. Thus, there has been a strong demand for a highly sensitive, quick response sensor material that works at room temperature with sufficient lifetime.

Recently, a wide band gap p-type semiconducting TeO$_2$ (3.8 eV) in a one-dimensional (1D) nanostructure form has been suggested as an ideal candidate for NO$_2$, NH$_3$, and H$_2$S gas-sensing applications at room temperature.[13-15] However, major drawbacks still hold further development due to difficulties in the mass production of reproducible high quality TeO$_2$ nanowires (NWs) used to construct metal-oxide-semiconductor based sensors. In addition, because the diameters of NWs influence the sensing performance significantly, the reported smallest diameter of ~ 200 nm so far may not be small enough to exploit the full sensing capability.[14, 15] In this report, we carefully optimized the growth conditions for synthesizing high-quality one-dimensional TeO$_2$ NWs by thermal evaporation using Au as a catalyst. We have successfully synthesized relatively uniform, high-density, and high-aspect-ratio TeO$_2$ NWs at a low temperature of 330 °C. We have produced the smallest diameter compared to those reported thus far, supporting the highest specific surface area and its enhanced intrinsic sensing property. Studies on the growth mechanism, structural properties, and hydrogen gas sensing properties are discussed in detail. The device fabricated by a

single TeO$_2$ NW has shown the highest responses of 57% and 138% at room temperature and at higher temperature ranges, with low power consumption. We identified three key factors that affect the overall performance of the hydrogen gas sensor: (1) extremely small size, (2) intrinsic p-type semiconducting property, and (3) hydrogen diffusion.

Experimental

NW Synthesis: A high-purity tellurium metal source (99.999%, mesh) (20 mg) purchased from Sigma-Aldrich was kept on an alumina plate, above which a silicon substrate coated with 3 nm thick gold catalyst was placed at a certain distance for NW growth. The alumina plate containing the tellurium source and the substrate was carefully transferred into a furnace. To determine the optimum conditions for producing high-quality TeO$_2$ NWs, three growth parameters were constantly monitored: distance, growth time, and temperature. We found that the optimized growth condition is 330 °C for 1 hr holding period with the source-substrate distance of 2 mm. The synthesized NWs were analyzed by field emission scanning electron microscopy (FE-SEM; JEOL JSM–7401F, Japan), high-resolution transmission electron microscopy (HRTEM; FE-TEM JEM2100F, Japan) and X-ray diffraction (XRD; D8 FOCUS 2200V, Bruker AXS, with Cu K$_\alpha$ radiation and nickel as K$_\beta$ filter. N$_2$ adsorption–desorption isotherms of TeO$_2$ NWs were also obtained using a Micrometrics ASAP 2000 to determine the specific surface area.

Device Fabrication and Measurement: The TeO$_2$ NWs were initially dispersed in ethanol by mild sonication and then dispersed on SiO$_2$/Si substrate. A device was then fabricated by a standard photolithography following the literature recipe.[16] The electrodes consisted of 50 nm thick titanium (as an adhesion promotion layer) and 150 nm thick gold. The devices were then cleaned by oxygen plasma with a flow rate of 30 sccm for 10 mins, rinsed in ethanol for 5 s, and finally dried in nitrogen gas.

The hydrogen sensing characteristics of TeO$_2$ NW-based device were investigated using a custom-designed H$_2$ sensing test chamber assembly. The test chamber assembly consisted of a mixing chamber connected to a main chamber (capacity ~5 L) via an inlet valve. The

main chamber consisted of an *in situ* heating arrangement with a maximum allowable temperature of 160 °C and accuracy of ±0.1 °C min^{-1}. The mixing chamber had two input valves, one for H$_2$ gas and the other for dry air,[17] which was used as a carrier gas. Mass-flow controllers were connected across the input terminals of the mixing chamber to control gas flow. The gases were withdrawn from the main chamber by opening an outlet valve connected through a baffle valve to an oil-sealed rotary pump. Initially, a low pressure of 5 mTorr was maintained in the main chamber to remove surface adsorbed organic molecules. Temperature was set to the desired value using a slow ramping rate of 10 °C min^{-1}. Temporal H$_2$ gas sensing characteristics were determined from the same device by applying a DC bias (1 Volt) across the fabricated TeO$_2$ NW device to verify the sensor stability at various hydrogen concentration including 1%, 0.5%, 2000 ppm, 100 ppm, and 10 ppm hydrogen concentrations at various testing temperatures.

Results and discussion

The surface morphology and size of as-grown NWs on substrates were investigated by FE-SEM as shown in Fig. 1 (a). Optimized conditions for high density, good morphology, and small diameter NW growth are 1 hr duration and 330 °C, at a distance of 2 mm between the substrate and source. TeO$_2$ NWs grown under optimized conditions have a relatively uniform diameter of 30~40 nm and are about 20 micrometers long. Increase in time or distance caused the formation of larger diameters, decreased aspect ratios, and larger particles.
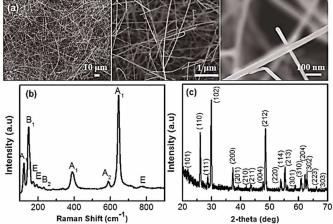

Fig. 1 (a) SEM image of TeO$_2$ NW growth under optimized conditions of 330 °C for 1 hr holding period at source substrate distance of 2 mm. (b) Raman spectra and (c) XRD pattern of TeO$_2$ grown on Au-coated Si (100) substrate.

The Raman spectra of as-grown TeO$_2$ were collected to confirm the phase and crystallinity of synthesized NWs, as shown in Fig. 1 (b). Tellurium dioxide has a tetragonal crystal structure in the P4$_1$2$_1$2 space group. The Raman peaks observed for TeO$_2$ NWs were in good agreement with the standard literature report of tetragonal α-TeO$_2$ in the crystalline phase.[18] α-TeO$_2$ has symmetry of 8E+4A$_1$+4A$_2$+5B$_1$+4B$_2$, in which A$_1$ and A$_2$+E+B$_1$ modes are Raman active. The strong Raman peak at 648 cm^{-1} corresponds to A$_1$ vibrational modes. The peak associated with B$_2$ mode was observed at 235 cm^{-1}.[17] The peak observed at 592 cm^{-1} is responsible for symmetric and anti-symmetric stretching modes of the TeO$_2$ molecular units. Asymmetric and symmetric (A$_1$) bending modes are observed

at 393 cm^{-1} and 110 cm^{-1}, respectively. The sharp B$_1$ bending mode is observed at 172 cm^{-1}. Sharp Raman peaks clearly indicate the high quality of as-grown TeO$_2$ NWs.

The X-ray diffraction pattern for as-grown TeO$_2$ NWs is shown in Fig. 1 (c). A scanning speed of 2°/min was used during the measurement. All peaks coincided well with the tetragonal tellurium dioxide crystalline phase. Lattice parameter values are estimated to be a = 4.796 Å, c = 7.626 Å, and α = β = γ = 90°, which are in good agreement with standard JCPDS data (JCPDS No.11-0693). The appearance of sharp peaks demonstrates that as-grown TeO$_2$ NWs are highly crystalline in nature.

The microstructure and single-crystallinity of as-grown TeO$_2$ NWs were characterized by TEM. The TEM image of TeO$_2$ NWs shown in Fig. 2 (a) demonstrates that NW surfaces are smooth. Detailed TEM analysis did not reveal any structural defects, such as stacking faults or dislocations in the NWs. SAED and HRTEM images obtained from TeO$_2$ NWs are shown in Fig. 2 (b) and (c), respectively. An index of the clear spots in the selected area diffraction (SAED) pattern clearly indicates that TeO$_2$ NWs are single crystalline and grow along the [102] direction.
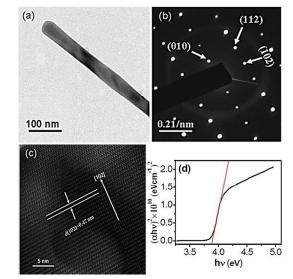

Fig. 2 (a) TEM image, (b) SAED pattern, (c) HRTEM image of TeO$_2$ NW, and (d) The Tauc plot of TeO$_2$ NW.

We also attempted to determine the bandgap of our TeO$_2$ NWs using Tauc plot from diffuse reflectance spectrum as shown in Fig. 2 (d). From the Tauc plot, we found that our NWs possess the band gap of 3.8 eV, which is in reasonable agreement with the value reported in literature.[13]

Temporal hydrogen response was measured using a single TeO$_2$ NW at different temperatures (25 °C, 60 °C, 80 °C, 100 °C, 120 °C, and 140 °C) under 0.5% and 1% H$_2$ concentrations. As shown in Fig. 3 (b) and (c), when hydrogen was introduced to the main chamber, a sudden rise with sheer ascending slope was observed. When the $\Delta R/R$ became saturated and as soon as hydrogen gas was turned off in the main chamber, a swift drop in the resistance change ratio was observed. The decrease in $\Delta R/R$ can be divided into two phases, a fast decrease and a

piece meal descending slope. The subsequent testing cycles repeatedly showed the same behavior.

Fig. 3 (a, b, c, e and f(inset)) shows the device structure and $\Delta R/R$ response as a function of time in a testing circuit according to the common resistance change ratio calculation formula.[19, 20] Temporal response characteristics were also compared with those of the typical materials used in gas sensors such as Pd NWs, GaN NWs, and SnO_2 NWs reported elsewhere,.[21-24] The rise and drop time defined as Δt_1 and Δt_2, shown in Fig. 3 (b), were found to be 100 s and 250 s, respectively, which are smaller than previously reported values.[21-23] F. Yang *et al.* reported that the response time and recovery time for Pd NW were about 350 s and 250 s for 0.5% and 1% H_2 concentration in air, whereas the recovery times were 250s and 270 s
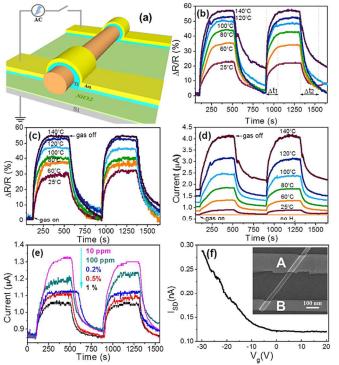

Fig. 3 (a) Schematic of the fabricated device. Plot of $\Delta R/R$ versus time for TeO_2 single NW device subjected to cyclic hydrogen unloading and loading at various working temperatures with (b) 1% H_2 and (c) 0.5% concentration. (d) Sensitivity of the TeO_2 single NW device with different temperatures at a H_2 1% concentration. (e) Current variation as a function of time for TeO_2 single NW device subjected to cyclic hydrogen unloading and loading at 60 °C with various concentrations. (f) I_{SD} vs V_g curve for the TeO_2 NW based field-effect transistor. (inset shows sensing device structure with electrode A and B)

respectively.[22] In SnO_2 NW case, G.W. Yang's group reported that longer than 250 s were observed for both response time and recovery time at 200 ℃ for 0.1% H_2 in air.[24] J. L. Johnson *et al* also reported that Pd-coated GaN NW showed up to 11 times enhancement compared to pure GaN NW, although the device was restored to almost 90% of the initial level within 2 mins. Based on this, the response time was estimated to be much longer than 7 minutes at room temperature.[21] In our investigation, a resistance change ratio of ∼ 25% at room

temperature and 57% at high temperature of 140 ℃ was obtained. It clearly shows that TeO_2 NWs exhibited a large resistance change at all the tested temperatures, which reveals its excellent selectivity for hydrogen gas in dry air as verified in Fig. 3 (c) and (d). In addition, 1 volt device operation indicates low power consumption.[24-26] The sensing properties of TeO_2 NWs were investigated, and their distinctive features are shown in Fig. 3 (b), (c) and (e). These figures indicate that higher working temperatures resulted in higher response, which is represented by the resistance ratio change and gas sensitivity. To find out the detection limit in ppm, we tested the TeO_2 NW based gas sensors at 2000 ppm, 100 ppm and 10 ppm hydrogen gas concentrations as shown in Fig. 3 (e). Based on this calculation,[27] we believe that our TeO_2 NW based hydrogen sensors have the detection limit of 20 ppm hydrogen gas concentration. For cycle stability, the same device up to 15 cycles were tested as shown in Fig. 3 (b, c, and e), and at 10 ppm as shown in Fig. 3 (e), the device returned to the original state, which indicated that our device exhibits reasonably good stability. Furthermore, the electrical resistance and resistivity at different test temperatures are given in table 1. We believe that three key factors are ascribed to contribute to the high sensitivity of our TeO_2 NWs based hydrogen sensors. First of all, having extremely small size is critically beneficial as gas-sensing ability can be greatly limited by low surface-to-volume ratio.[28]

Table 1. Electrical resistance and resistivity of the TeO_2 NW at various testing temperatures.

Temperature: (℃)	25 ℃	60 ℃	80 ℃	100 ℃	120 ℃	140 ℃
Resistance: R ($\times 10^6 \Omega$)	1.45	1.17	0.95	0.81	0.66	0.56
Resistivity: ρ ($\times 10^{-3} \Omega \cdot m$)	4.46	3.60	2.92	2.49	2.03	1.72

In our experiment, NWs synthesized using gold as a catalyst not only had lower synthetic temperature and energy consumption, but also higher surface-to-volume ratio (around 9 $\times 10^7$).[29] N_2 adsorption–desorption isotherms of TeO_2 NWs were obtained to determine the specific surface area using a Micrometrics ASAP 2000 at −196 ∘C (liquid N_2) as shown in Fig. 4 (a). Specific surface area (SSA) was estimated to be 137.45 m^2/g based on Brunauer–Emmett–Teller theory. The diameters of TeO_2 NWs reported by Liu *et al.* were distributed around 200 nm,[30] whereas the TeO_2 NWs used for this study have diameters uniformly located in the range of 30 to 40 nm. This small size will greatly enhance the sensing properties of devices.[31, 32] After maintaining in vacuum, surface-chemisorbed organic molecule is released to the air upon exposure to reductive H_2 gas. TeO_2 NWs chemically attract H_2 molecules to reduce surface tension by forming strong hydrogen bonds with oxygen atoms on NWs. This adsorption force is especially crucial for small molecular hydrogen atoms. During this process, electrons tend to approach close to H atoms to fulfill the outer K electron orbital and form the most stable state. Free electron carriers were trapped by chemisorbed H_2 gas molecules, which behave in the same way as acceptors. Secondly, intrinsic p-type semiconducting property is also

important. In principle, current decreases for n-type semiconducting materials due to decreases in the electron concentration of the semiconducting material. For p-type semiconductors, current increases due to the combination of electrons with holes released from redox reactions. This creates a situation in which electrons are caught by surface attachment.[19] Current increased upon switching on reductive gas in this experiment, confirming the p-type behavior of TeO_2 in nanoscale. TeO_2 NW based field-effect transistor was fabricated to confirm a p-type semiconducting behavior as shown in Fig. 3 (f). Lastly, we believe that hydrogen atoms at relatively high temperatures gain adequate kinetic energy to diffuse inside the TeO_2 tetragonal structure due to the small covalent radius of hydrogen, which is approximately 31 picometers. TeO_2 lattice can readily absorb a large amount of target hydrogen gas, depending on temperature.[26, 33, 34] Both the surface and inside of NWs influences the resistance ratio change,[28] leading to higher gas sensitivity at higher temperatures. In the gas-off state, the pressure difference in hydrogen gas outside and inside the NWs is quite significant. This causes hydrogen to move quickly, illustrating why a swift drop in resistance change ratio appeared. After this drop, the decreasing hydrogen gas pressure difference slows down the relative moving speed of H atoms. This results in a piecemeal descending slope, as shown in Fig. 3 (b) and (c). At higher temperatures, hydrogen diffusion plays a more significant role. To confirm whether our TeO_2 NW conferred higher sensitivity at higher temperatures, we studied variations in the percentage change of the device as a function of temperature, as shown in Fig. 4 (b). The percentage change was calculated using equation (1):
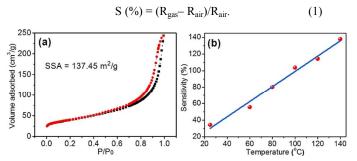
$$S (\%) = (R_{gas} - R_{air})/R_{air}. \qquad (1)$$

Fig. 4 (a) N_2-isothem of TeO_2 NWs produced by using gold as a catalyst based on thermal evaporation method. (b) Percentage change of TeO_2 single NW device with different temperatures at H_2 concentration of 1%.

This examination revealed that the TeO_2 single NW device works well under ambient conditions and the escalating trend indicate the stability of TeO_2 based gas sensor at higher temperatures. At the same time, its sensitivity increases with increasing temperatures (60 ˚C, 80 ˚C, 100 ˚C, 120 ˚C, and 140 ˚C).

Conclusions

Herein, we report a reliable method for producing small, and reproducible high quality TeO_2 NWs using a simple thermal evaporation without any post annealing process. Raman spectrum, XRD and TEM techniques were used to characterize the quality of TeO_2 NWs and to disclose their ultrahigh

hydrogen sensing properties at room temperature and at other tested temperatures (60 ˚C, 80 ˚C, 100 ˚C, 120 ˚C, and 140 ˚C) under 0.5% and 1% H_2 concentrations. The obviously large percentage change in $\Delta R/R$ between each temperature implies that TeO_2 NWs based hydrogen sensors also perform well when operating at higher temperatures. The exact sensitivity values of $\Delta R/R$ responses were 28% and 57% at 25 ˚C and 140 ˚C, respectively, for 0.5% H_2 concentration. The detection limit was estimated to be 23 ppm based on our sensitivity test. Sensitivity-versus-temperature analysis revealed that sensitivity reached up to 138% at 140 ˚C for 1% H_2 gas concentration. Because of the reliable synthesis, good stability, cost-effective fabrication, quick response and high sensitivity, TeO_2 NW based hydrogen sensor devices will likely play an important role in H_2 gas sensor applications in the near future.

Notes and references
a Department of Physics, Institute of Basic Sciences, SKKU Advanced Institute of Nanotechnology, Sungkyunkwan University, 300 Cheoncheon-dong, Jangan-gu, Suwon 440-746, South Korea

Fax: +82-31-290-5947; Tel: +82-31-290-5906; Email: djkang@skku.edu.

b Department of Electrical and Computer Engineering, McGill University, 3480 University Street, Montreal, Quebec H3A 2A7, Canada

1. R. A. Potyrailo and V. M. Mirsky, *Chem. Rev.,* 2008, **108**, 770.
2. A.M. Azad, S.A. Akbar, S.G. Mhaisalkar, L.D. Birkefeld and K.S. Goto, *J. Electrochem. Soc.,* 1992, **139**, 3690.
3. G. Eranna, B.C. Joshi, D.P. Runthala and R.P. Gupta, *Cristal Rev. Solid State Mater. Sci.,* 2004, **29**, 111.
4. A. Kolmakov and M. Moskovits, *Annu. Rev. Mater. Res.,* 2004, **34**, 151.
5. M. Zhao, J.X. Huang and C.W. Ong, *Sensors and Actuators B*, 2014, **191**, 711.
6. J. Kukkola, M. Mohl, A.R. Leino, J. Mäklin, N. Halonen, A Shchukarev, Z. Konya, H. Jantunen and K. Kordas, *Sensors and Actuators B*, 2013, **186**, 90.
7. E.M. El-Maghraby, A. Qurashi and T. Yamazaki, *Ceramics International*, 2013, **39**, 8475.
8. N. V. Long, M. Yuasa, C. M. Thi, Y.Q. Cao, Y. Yang, T. Nann and M. Nogami, *RSC Adv.*, 2013, DOI: 10.1039/C3RA46410E.
9. J.M. Ma, L. Mei, Y.J. Chen, Q.H. Li, T.H. Wang, Z. Xu, X.C. Duan and WJ.. Zheng, *Nanoscale*, 2013, **5**, 895.
10. M.R. Vaezi and S.K. Sadrnezhaad, *Mater. Sci. Eng. B.,* 2007, **140**, 73.
11. T. Siciliano, A. Tepore, G. Micocci, A. Serra, D. Manno and E. Filippo, *Sens. Actuators B,* 2008, **133**, 321.
12. I. Ray, S. Chakraborty, A. Chowdhury, S. Majumdara, A. Prakash, R. Pyare and A. Sen, *Sens. Actuators B*, 2008, **130**, 882.

13. T. Siciliano, A. Tepore, G. Micocci, A. Genga, M. Siciliano and E. Filippo, *Sensors and Actuators B,* 2009, **138**, 207.

14. Z. F. Liu, T. Yamazaki, Y. B. Shen, T. Kikuta, N. Nakatani and T. Kawabata, *Appl. Phys. Lett.,* 2007, **90**, 173119.

15. T. Siciliano, M. D. Giulio, M. Tepore, E. Filippo, G. Micocci and A. Tepore, *Sensors and Actuators B,* 2009, **137**, 644.

16. O. Lupan, L. Chow and G. Chai, *Sens. Actuators B: Chem.,* 2009, **141**, 511.

17. G. F. Fine, L. M. Cavanagh, A. Afonja and R. Binions, *Sensors,* 2010, **10**, 5469.

18. A.P. Mirgorodsky, T. Merle-Méjean. J. C. Champarnaud, P. Thomas and B. Frit, *J. Phys. Chem. Solids,* 2000, **61**, 501.

19. V. V. Sysoev, J. Goschnick, T. Schneider, E. Strelcov and A. Kolmakov, *Nano Lett.,* 2007, **7**, 3182.

20. E. R. Waclawik, J. Chang, A. Ponzoni, I. Concina,D. Zappa, E. Comini, N. Motta, G. Faglia and G. Sberveglieri, *Beilstein J. Nanotechnol.,* 2012, **3**, 368.

21. J.L. Johnson, Y. Choi, A. Ural, W. Lim, J.S. Wright, B.P. Gila,F. Ren and S.J. Pearton, *J. Electron. Mater.,* 2009, **38**, 490.

22. F. Yang, S. C. Kung, M. Cheng, J. C. Hemminger and R. M. Penner, *ACS Nano.,* 2010, **4**, 5233.

23. B. L. Huy, S. Kumar and G. H. Kim, *J. Phys. D:Appl. Phys.,* 2011, **44**, 325402.

24. B. Wang, L. F. Zhu, Y. H. Yang, N. S. Xu and G. W. Yang, *J. Phys. Chem. C,* 2008, **112**, 6643.

25. F. Yang, D. K. Taggart and R. M. Penner, *Nano Lett.,* 2009, **9**, 2177.

26. X. Q. Zeng, M. L. Latimer, Z. L. Xiao, S. Panuganti, U. Welp, W. K. Kwok and T. Xu, *Nano Lett.,* 2011, **11**, 262.

27. S.B. Cai, Y. Zhang and Z. M. Duan, *J. Micromech. Microeng.* 2012, **22**, 125017.

28. K. J. Jeon, M. H. Jeun, E. Lee, J. M. Lee, K. Lee, P.V. Allmen and W. Y. Lee, *Nanotechnology,* 2008, **19**, 495501.

29. H. Pan and P. F. Yuan, *ACS Nano.,* 2008, **2**, 2410. Surface to volume ratio in our case was estimated assuming TeO_2 NW has the cylinder like cross-section: Surface area: $S = 2\pi r^2 + 2\pi rh = 2.8 \times 10^{-12}$ m^2, Volume: $V = \pi r^2 h = 3.18 \times 10^{-20}$ m^3. Where, r and h stand for diameter and length of TeO_2 NW. Therefore, Surface-to-volume ratio $= S/V = 9 \times 10^7$.

30. Z. F. Liu, T. Yamazaki, Y. B. Shen, T. Kikuta and N. Nakatani, *Jpn J. Appl Phys.,* 2008, **47**, 771.

31. L. Liao, H.B. Lu, J.C. Li, H. He, D.F. Wang, D.J. Fu, and C. Liu, *J. Phys. Chem. C*, 2007, **111**, 1900.

32. M. Tonezzer and N.V. Hieu, *Sensors and Actuators B*, 2012, **163**, 146.

33. J. M. Baik, M. H. Kim, C. Larson, C. T. Yavuz, G. D. Stucky, A. M. Wodtke and M. Moskovits, *Nano Lett.,* 2009, **9**, 3980.

34. J. Robertson, *J. Phys. C: Solid State Phys.*, 1979, **12**, 4767.